Polymer multilayer tattooing for enhanced DNA vaccination

Citation: DeMuth, Peter C., Younjin Min, Bonnie Huang, Joshua A. Kramer, Andrew D. Miller, Dan H. Barouch, Paula T. Hammond, and Darrell J. Irvine. "Polymer Multilayer Tattooing for Enhanced DNA Vaccination." Nature Materials 12, no. 4 (January 27, 2013): 367–376.

As Published: http://dx.doi.org/10.1038/nmat3550

Publisher: Nature Publishing Group

Persistent URL: http://hdl.handle.net/1721.1/91478

Version: Author's final manuscript: final author's manuscript post peer review, without publisher's formatting or copy editing

Published in final edited form as:
Nat Mater. 2013 April ; 12(4): 367–376. doi:10.1038/nmat3550.

Polymer multilayer tattooing for enhanced DNA vaccination

Peter C. DeMuth[1], **Younjin Min**[2], **Bonnie Huang**[1], **Joshua A. Kramer**[3], **Andrew D. Miller**[3], **Dan H. Barouch**[4,8], **Paula T. Hammond**[2,5,6], and **Darrell J. Irvine**[1,5,6,7,8,9]

[1]Department of Biological Engineering, Massachusetts Institute of Technology (MIT), Cambridge, MA, USA

[2]Department of Chemical Engineering, MIT, Cambridge, MA, USA

[3]New England Primate Research Center, Harvard Medical School, Southborough, MA, USA

[4]Division of Vaccine Research, Beth Israel Deaconess Medical Center, Harvard Medical School, Boston, MA, USA

[5]Institute for Soldier Nanotechnologies, MIT, Cambridge, MA, USA

[6]Koch Institute for Integrative Cancer Research, MIT, Cambridge, MA, USA

[7]Department of Materials Science and Engineering, MIT, Cambridge, MA, USA

[8]Ragon Institute of MGH, MIT, and Harvard, Boston, MA, USA

[9]Howard Hughes Medical Institute, Chevy Chase, MD, USA

Abstract

DNA vaccines have many potential benefits but have failed to generate robust immune responses in humans. Recently, methods such as *in vivo* electroporation have demonstrated improved performance, but an optimal strategy for safe, reproducible, and pain-free DNA vaccination remains elusive. Here we report an approach for rapid implantation of vaccine-loaded polymer films carrying DNA, immune-stimulatory RNA, and biodegradable polycations into the immune-cell-rich epidermis, using microneedles coated with releasable polyelectrolyte multilayers. Films transferred into the skin following brief microneedle application promoted local transfection and controlled the persistence of DNA and adjuvants in the skin from days to weeks, with kinetics determined by the film composition. These “multilayer tattoo” DNA vaccines induced immune responses against a model HIV antigen comparable to electroporation in mice, enhanced memory T-cell generation, and elicited 140-fold higher gene expression in non-human primate skin than intradermal DNA injection, indicating the potential of this strategy for enhancing DNA vaccination.

DNA vaccines have been intensively studied due to potential advantages such as ease of GMP production, lack of anti-vector immunity, and capability to promote both cellular and humoral immune responses.[1,2] However, plasmid DNA (pDNA) immunization has shown poor efficacy in non-human primates and human trials,[1,3] and the most promising methods

Correspondence should be addressed to P.T.H (hammond@mit.edu) and D.J.I. (djirvine@mit.edu).

Author Contributions

P.C.D., P.T.H., and D.J.I. designed the experiments. P.C.D., D.H.B., and D.J.I. designed macaque skin studies. P.C.D. carried out the experiments; Y.M. assisted in *in vitro* nucleic acid release studies. B.H. synthesized the PNMP polymers. A.D.M. and J.A.K. collected the macaque skin. P.C.D, P.T.H, and D.J.I. analyzed the data and wrote the paper.

Competing Financial Interests

None.

for increasing the potency of these vaccines have employed involved methods such as *in vivo* electroporation that are not attractive for widespread prophylactic vaccination.[4] Parallel to the technical challenges of DNA vaccination, traditional needle-based administration of vaccines has a number of disadvantages: liquid vaccine formulations typically require refrigeration that raise the costs and complexity of global distribution (the "cold chain"),[5] administration requires trained personnel, and safety is hampered by needle re-use and needle-based injuries.[6] These issues become particularly acute for vaccine distribution in the developing world.[6–8]

We hypothesized that DNA vaccine delivery would be substantially enhanced by an approach that could simultaneously (i) target DNA to tissues rich in immune-response-governing dendritic cells, (ii) promote sustained transfection without toxicity, (iii) and provide supporting inflammatory cues to enhance the induction of a potent immune response. In addition, vaccines have been shown to vary widely in potency depending on the kinetics of both antigen and adjuvant exposure, with optimal immunity often stimulated by persistence of antigen and inflammatory signals for up to one week.[9–12] To meet these design goals, we developed a strategy using microneedles to rapidly implant into the skin biodegradable polymer films, which continuously release DNA polyplexes and adjuvant molecules in this immunologically-competent tissue over a tunable and sustained period of time. We show that skin-implanted vaccine multilayers allow control over the physical and functional persistence of inflammatory adjuvants and pDNA, efficiently transfecting cells in murine skin and eliciting cellular and humoral immune responses comparable to or exceeding *in vivo* electroporation of pDNA, one of the most promising current technologies for DNA vaccine delivery.[4] We have termed this approach of implanting persistent polymer films into the skin 'multilayer tattooing', by analogy to conventional tattooing where persisting inks are deposited in the skin. These multilayer vaccine formulations allow for dry-state storage of coated microneedle patches at room temperature for weeks without loss of activity, an important advantage for decreasing costs and improving vaccine availability in remote areas. Further, when applied to viable macaque skin *ex vivo*, multilayer tattooing elicited 140-fold greater gene expression compared to naked DNA injection. Thus, this polymer film tattooing approach may offer a route to efficacious DNA vaccines via a pain-free and self-administrable dry skin-patch platform.

Design, fabrication, and testing of 'quick-release' multilayers

We first set out to create implantable vaccine coatings using polyelectrolyte multilayers[13,14] (PEMs, Fig. 1a), nanostructured films formed by iterative adsorption of alternately-charged polymers, which embed large weight-fractions of biologic cargos (e.g., DNA, up to 40% of total film mass),[15] stabilize embedded molecules in the dried state,[16,17] and exhibit release kinetics predetermined by the film architecture/composition. We hypothesized that rapid multilayer transfer from coated microneedles into the epidermis could be achieved via an underlying polymer film designed to instantly dissolve when microneedles are applied to the skin (Fig. 1b), allowing the kinetics of DNA/adjuvant release in the tissue to be tailored separately from the time required for a microneedle patch to be kept on the skin. To create such releasable vaccine coatings, we employed a photo-sensitive and pH-responsive polymer, Poly(o-Nitro-benzyl-methacrylate-*co*-Methyl-methacrylate-*co*-Poly(ethylene-glycol)-methacrylate) (PNMP), for the release-layer. PNMP is initially organic-soluble, but on brief exposure to UV, cleavage of the o-nitrobenzyl groups converts the polymer to a weak polyelectrolyte (*uv*-PNMP) soluble in water above pH ~6.5.[18] As shown below, this photo-switchable solubility provided the means to prove that PEM film implantation depended on PNMP release-layer dissolution.

Skin patches were fabricated by melt-molding poly(L-lactide) (PLLA) on poly(dimethyl-siloxane) (PDMS) molds to obtain arrays of microneedles each 250 μm in diameter at their base and 650 μm in height (Supplementary Fig. S1).[19] Biotinylated-PNMP (bPNMP, Supplementary Fig. S2a) films were coated on microneedles by spray deposition[20] from 1,4-dioxane solutions, UV-exposed to trigger the photochemical transition in the film, and then stained with fluorescent streptavidin (SAv) to permit visualization of the release-layer by microscopy. Next, LbL deposition was used to construct an overlying PEM film composed of Cy5-labeled pDNA encoding luciferase (Cy5-pLUC) and the transfection agent poly-1, a biodegradable poly(β-amino-ester) (PBAE, Supplementary Fig. S2b).[19,21] PEM films were initiated by depositing 20 bilayers of protamine-sulfate (PS) and poly(4-styrene-sulfonate) (SPS) to provide a uniform charge density, followed by iterative adsorption of poly-1 and Cy5-pLUC (Fig. 2a). Profilometry measurements performed on PEMs constructed in parallel on Si substrates showed linear multilayer growth with increasing deposition cycles as previously reported for (PBAE/pDNA) films (Fig. 2b).[19,21] Confocal imaging of microneedles coated with composite (*uv*-bPNMP)$(PS/SPS)_{20}$(poly-1/Cy5-pLUC)$_{35}$ PEM films showed conformal co-localized fluorescence from SAv-labeled *uv*-bPNMP and Cy5-pLUC over the surface of each PLLA microneedle (Fig. 2c). (Individual *uv*-bPNMP and PEM films were too thin to resolve as distinct layers). When analyzed at sequential stages of PEM film deposition, the mean total SAv-bPNMP fluorescence signal from single microneedles was stable but Cy5-pLUC fluorescence linearly increased with increasing rounds of bilayer deposition, confirming linear film growth on microneedles (Fig. 2d). Measurement of DNA recovered from microneedle coatings disrupted by treatment with sodium chloride showed ~4.2μg DNA deposited per bilayer per cm^2 of the microneedle array (Fig. 2d). Sequential assembly of PEM films comprising layers of (poly-1/poly(I:C)) followed by layers of (poly-1/pLUC) generated microneedles coated with complete vaccine multilayers containing pDNA, a transfection agent, and a strong adjuvant (Fig. 2e). These composite films showed conformal coating of both vaccine components (Fig. 2f) and linear growth of pLUC layers over poly(I:C) layers with increasing number of deposition cycles (Fig. 2g, h). Key to this process is that the DNA-containing PEM is never exposed to UV-irradiation, thus avoiding any potential damage due to UV exposure.

Lack of toxicity/biocompatibility is critical for materials used in prophylactic vaccines, and the components of the microneedle system were chosen with biocompatibility in mind: polylactide used as the microneedle base is a bioresorbable polymer with a long history of clinical use in resorbable sutures and drug delivery devices. Although we chose to use (PS/SPS) 'base-layer' films for convenience in lab-scale studies, simplified film architectures composed of only PNMP and (PBAE/nucleic acids) could be deposited with linear growth per deposition cycle for 20 or more bilayers (data not shown). Previous studies have demonstrated the biocompatibility of both PNMP *in vitro*[18,22] and poly-1 and poly-2 polymers *in vitro* and *in vivo*.[23–25] Consistent with these data, we observed no apparent local toxicity in any of the mice treated throughout these studies.

Multilayer delivery into skin from microneedles

To test PEM film release from microneedle arrays, dried composite (SAv-labeled *uv*-bPNMP)$(PS/SPS)_{20}$(poly-1/Cy5-pLUC)$_{35}$ coatings (referred to henceforth as PNMP/PEM films) on microneedles were immersed in pH 7.4 PBS for varying times *in vitro* and imaged by confocal microscopy to quantitate *uv*-bPNMP and Cy5-pLUC fluorescence remaining on the microneedle surfaces. After 15 minutes incubation in PBS, we observed a significant loss of both bPNMP and Cy5-pLUC fluorescence from microneedle arrays (Supplementary Fig. S3). By contrast, no film release was observed if PEMs were assembled onto PNMP coatings that had not been irradiated to photo-switch the release-layer's solubility. To determine whether microneedles coated with releasable films would permit rapid multilayer

implantation *in vivo*, we applied dry (PNMP/PEM)-coated microneedles to the auricular skin of C57Bl/6-MHC II-GFP mice.[26] Trypan blue staining of treated skin in this case showed consistent microneedle insertion (Fig. 3a). Mirroring our *in vitro* observations, confocal imaging of microneedles after 15 minutes application to murine skin showed that both *uv*-bPNMP and Cy5-pLUC fluorescence was rapidly lost from coated microneedles, but only if PNMP films were irradiated before multilayer assembly to prime for rapid dissolution of the release-layer (Fig. 3b, c). Confocal imaging of skin samples following application of (PNMP/PEM)-coated microneedles for 15 minutes showed significant transfer of Cy5-pLUC in the epidermis co-localized with MHC II-GFP$^+$ Langerhans cells (LCs) (Fig. 3d) and up to 400 μm deep into the skin (Fig. 3e), but only when the PNMP layer was UV-primed. Similarly, microneedles carrying poly(I:C)-loaded PEM films deposited fluorescently-labeled poly(I:C) into the skin, colocalizing in the same z-plane with MHC II-GFP-expressing cell populations (Figs. 3f). Twenty-four hours after implantation of (poly-1/nucleic acid) multilayers, the degrading films were observed dispersed into the tissue around the needle insertion site and showed apparent uptake in colocalized LCs (Fig. 3g). Thus, the *uv*-PNMP release-layer promotes rapid transfer of DNA- or RNA-loaded films from microneedles into the skin.

Control over nucleic acid persistence and activity in skin via implanted multilayer composition

We next tested whether the *in vivo* kinetics of nucleic acid release into the surrounding tissue could be controlled via the composition of multilayers implanted in the skin. Past studies have demonstrated the ability of multilayers composed of pDNA assembled with the PBAEs poly-1 or poly-2 to mediate release with varying kinetics.[27,28] Consistent with this prior work, $(PS/SPS)_{20}(poly\text{-}1/poly(I:C))_{35}$ and $(PS/SPS)_{20}(poly\text{-}1/pLUC)_{35}$ multilayers constructed on Si substrates exhibited rapid release at 37°C of ~80% pLUC or poly(I:C) within 24 hours, while analogous films constructed with poly-2 showed a slower release lasting ~1 week (Supplementary Fig. S4). To determine whether the composition of PBAE multilayers implanted via microneedle delivery could mediate similar tunable release of nucleic acid therapeutics *in vivo*, we constructed (PBAE/Cy5-poly(I:C)) PEM films on *uv*-PNMP-coated microneedles using poly-1 or poly-2 as the PBAE component. Following application of coated microneedles to the skin of C57Bl/6 mice for 15 min, we monitored the fluorescence signal of implanted Cy5-poly(I:C) over time using whole-animal fluorescence imaging. Similar to the *in vitro* trend, films encapsulating poly(I:C) with poly-1 were quickly cleared from the application site, while (poly-2/poly(I:C)) films persisted for 10 days following application (Fig. 4a). To quantify the functional impact of sustained polyI:C adjuvant release *in vivo*, we applied microneedles carrying (poly-2/poly(I:C)) multilayers to the auricular skin of mice or injected equivalent doses of free poly(I:C) intradermally at the same site, and administered the chemiluminescent probe luminol to trace local inflammation over time. Systemically-injected luminol emits photons when catabolized by myeloperoxidase (MPO) produced by activated innate immune cells at sites of inflammation.[29,30] As shown in Fig. 4b, bolus poly(I:C) injection elicited a transient burst of inflammation that resolved by 48 hr, while multilayer implantation resulted in 2-fold higher peak MPO activity at 24 hr that decayed slowly to baseline over ~1 week. Importantly, poly(I:C)-triggered inflammation was highly localized to the application site, as no elevation of systemic cytokines was observed following multilayer implantation (data not shown). Thus, the composition of implanted PEM films can directly control the kinetics of release and local inflammatory response in the skin.

The selection of poly-1 and poly-2 as biodegradable polycation components of these PEM coatings was motivated not only by their ability to regulate nucleic acid release, but also to

directly promote transfection by forming pDNA polyplexes *in situ* during film degradation.[21,31] Dynamic light scattering analysis of supernatants collected from these eroded films *in vitro* revealed large aggregates (50–300nm, data not shown), consistent with previous evidence of *in situ* polyplex formation/release from degrading (PBAE/pDNA) multilayers.[27,31] To determine whether controlled polyplex release from implanted films would allow gene expression kinetics to be regulated *in vivo*, we used bioluminescence imaging to monitor expression of luciferase-encoding DNA longitudinally in live animals. Although *in vivo* optical imaging analysis of bioluminescent signals is limited by variable photon penetration from different tissue depths and locations, it is useful for accurate comparison of relative signal from identical tissue sites and for longitudinal analysis of the duration of expression. Microneedles were prepared with (PNMP/PEM) coatings containing pLUC as before, with or without UV-priming of the PNMP release-layer. We verified that pDNA released from multilayers *in vitro* retained bioactivity over the entire course of film degradation comparable to fresh PBAE/DNA polyplexes (Supplementary Fig. S5). *In vivo*, control microneedles (where the release-layer was not UV-primed) applied to the skin of mice for 15 min led to no detectable expression of pLUC by bioluminescence imaging (Supplementary Fig. S6), consistent with the lack of detectable film transfer into skin under this condition. By contrast, mice treated with microneedles coated with (*uv*-PNMP/PEM) films showed significant levels of bioluminescence one day after application, demonstrating transfection of cells *in situ* (Fig. 4c). Further, the kinetics of pLUC expression varied greatly depending on the PBAE used: delivery of (poly-1/pLUC) multilayers led to luciferase expression that peaked after 3 days and declined to background levels after 10 days, while implantation of slower-degrading (poly-2/pLUC) films showed prolonged bioluminescence, peaking on day 3 then slowly decreasing to background levels by day 22 (Fig. 4c). Together this data shows that, multilayer tattooing can be used to tailor the duration of both inflammatory signals and antigen-encoding DNA expression *in vivo*, via selection of constituent polymers with varying degradation rates.

Embedding bioactive molecules in multilayer films has previously been shown to enhance their stability for dry-state storage at room temperature,[16,17] an attractive feature for vaccines given the costs and availability limitations imposed by the need for refrigeration of liquid vaccine formulations. To test whether (PBAE/pDNA) multilayer films coated on microneedles stabilize their DNA cargo for dry storage, we fabricated microneedle arrays coated with (*uv*-PNMP/PEM) films and stored them dry at 25°C for 0, 14, or 28 days before application to the skin of mice as before. Bioluminescence imaging of these animals after treatment revealed no significant decrease in transfection resulting from storage, indicating the maintenance of pDNA bioactivity in multilayers for extended durations (Fig. 4d). These results suggest that microneedles coated with vaccine-containing multilayers could be easily packaged for inexpensive dry-state storage and transportation to remote areas of the world, bypassing the ‘cold-chain’ requirements of conventional vaccines.

Enhanced DNA vaccine responses via microneedle-implanted multilayers

Previous work has demonstrated DNA uptake in both keratinocytes and local APCs following delivery to the skin in both humans and mice, both of which can contribute to induction of immune responses in DNA vaccination (reviewed in [32]). To test the ability of multilayer tattooing with vaccine-loaded polymer films to enhance DNA immunization, we coated microneedles with (*uv*-PNMP)(PS/SPS)$_{20}$(poly-1/poly(I:C))$_{35}$(poly-1/pGag)$_{35}$ composite releasable multilayers containing the adjuvant poly(I:C) and pGag, a plasmid encoding the model HIV antigen SIV-*gag* (Fig. 5a). We compared multilayer tattooing to several control immunizations using the same delivered dose of pGag and poly(I:C): injection of “naked” pDNA, the most common experimental strategy for DNA immunization in mice and humans; and *in vivo* electroporation, where DNA is administered

in the presence of an electric field to promote DNA uptake.[4,33] To confirm the importance of the pH-responsive release-layer, we also tested microneedles where the PNMP layer was not UV-treated, and hence unable to dissolve upon skin insertion. Finally, we also compared immune responses in mice receiving intradermal injections of poly-1/pGag polyplexes, to determine the importance of the sustained-release multilayer film architecture for generating immunity. In all cases we immunized groups of animals on days 0 and 28 with 20 μg pGag and 10 μg poly(I:C). Multilayer tattooing was performed with microneedles (MN ± UV) applied to the dorsal ear skin for 15 min. Control mice were injected intradermally (ID and ID Polyplex) in the ear skin, or intramuscularly with or without *in vivo* electroporation (IM ± EP). Peptide-MHC tetramer staining of peripheral blood mononuclear cells showed that IM and ID ± Polyplex administration produced only weak antigen-specific $CD8^+$ T cell responses (Fig. 5b-d). By contrast, microneedle-treated groups showed robust expansion of Gag-reactive T-cells exceeding 5% of the circulating $CD8^+$ population two weeks following the boost, a response that was quantitatively similar to frequencies observed for IM + EP immunized mice (Fig. 5b-d). Notably, the response to MN vaccination was ablated if the PNMP release-layer was not UV-treated (and was therefore unable to dissolve on application). Additionally, compared to all of the other vaccination regimens, microneedle administration generated substantially greater frequencies of $CD44^+CD62L^+$ central memory T-cells, a population thought to be important for recall immunity and long-term protection (Fig. 5e-f).[34] Following injection of naked pDNA 3.5 months after the prime to test recall responses, large frequencies of IFN-γ-producing $CD8^+$ T-cells were elicited (Fig. 5g), suggesting the establishment of robust T-cell memory. Finally, two weeks following the boost, we measured total Gag-specific IgG titers in sera and observed a 10-fold increase in microneedle treated mice over those given any other immunization regimen ($P < 0.01$, Fig. 5h). Thus, DNA vaccination via multilayer tattooing shows the potential to match (or exceed) the potency of *in vivo* electroporation, using a skin patch that can be stored in a dry state, is painlessly applied with no extraneous apparatus, and could be self-applied in minutes.

Enhanced transfection of non-human primate skin

While naked DNA injections stimulate immune responses in small animals, responses observed in non-human primates and humans have been much weaker.[1–3] To determine whether multilayer tattooing could also enhance the efficacy of DNA delivery in non-human primates, we tested the ability of PNMP-coated microneedles to deliver (poly-1/pLUC) multilayers into fresh explanted skin from Rhesus macaques *ex vivo*. Trypan blue staining and histological sectioning of macaque skin treated with uncoated PLLA microneedles showed uniform patterns of microneedle insertion into the superficial layers of the skin without disruption of underlying dermal layers or capillary vessels (Fig. 6a, b). We tested the ability of microneedles coated with (*uv*-PNMP/PEM) films to transfect *ex vivo* cultured macaque skin explants compared to intradermal injections of equivalent doses of naked pDNA. Microneedles coated with (PNMP/PEM) multilayers effectively transfected macaque skin explants following a 15 min application period, but as in mice, transfection only occurred if the PNMP release-layer was UV-primed for dissolution (Fig. 6c). Bioluminescence imaging of the treated skin samples showed that microneedle delivery generated consistent expression of luciferase at 140-fold greater levels compared to intradermally-injected naked DNA controls for several days ($P < 0.01$, Fig. 6d). Previous results in mice have indicated that the magnitude of gene expression following DNA vaccination correlates with the strength of T-cell responses *in vivo*.[35] Thus, although the limitations of *ex vivo* skin explant culture prevent measurement of the long-term duration of gene expression, these results indicate that microneedle delivery promotes strong initial DNA expression in non-human primate skin, where naked DNA injection elicits very weak transfection only a few fold above background. Although the magnitude of gene expression

is only one parameter determining the ultimate strength of immune responses following DNA vaccination, the ability to improve expression levels in primates is a significant result given that poor transfection efficiency is an acknowledged obstacle for improving DNA immunogenicity in large animal models and humans.[33,36]

Microneedles have recently shown substantial promise in vaccine delivery,[37,38] and several reports have begun to explore the use of metal microneedles to deliver DNA into the skin.[39–42] These studies have demonstrated the ability of naked DNA delivery by microneedles to provide enhanced immune responses compared to intramuscular injection, but only one study compared microneedle administration to alternative approaches designed to elicit improved transfection; in that test microneedles elicited T-cell responses comparable to gene gun delivery of DNA if twice the DNA dose was given by the microneedle array.[40] Here we have demonstrated a new approach for DNA vaccination via multilayer "tattooing", using microneedles employing a pH-responsive release-layer to rapidly implant biodegradable vaccine-loaded polymer films into the skin. (Note that this new approach should not be confused with prior studies of "DNA tattooing", where DNA solutions are literally applied to the skin using a commercial tattoo device[9,33,43]– a completely different method.) Multilayer tattooing simultaneously addresses several issues in DNA vaccine delivery: implanted multilayers deliver DNA with transfection agents, promoting transfection *in situ*; molecular adjuvants are co-delivered to amplify the immune response; and we have shown that the multilayer structure allows the kinetics of vaccine release to be tailored over days to weeks. Combined, these features enabled multilayer tattooing to elicit immune responses in mice far exceeding naked DNA injections. These responses were also comparable to *in vivo* electroporation, an approach currently viewed as a gold standard for experimental DNA vaccine potency but which requires special equipment, elicits pain and discomfort in recipients,[44,45] and is unlikely to be feasible in widespread prophylactic vaccination. Notably, vaccines have been shown to vary widely in potency based on the duration of exposure to antigen and adjuvant combinations.[9–12] Our studies suggest that the continuous release of polyplexes from implanted multilayers may be critical to the enhanced immunogenicity of multilayer tattooing, as bolus injection of free polyplexes formed from the same components elicited very weak immune responses. Finally, we have shown that formulation of DNA vaccines as multilayer coatings on microneedles provides the opportunity for long term maintenance of DNA bioactivity in a dried state without refrigeration, addressing cost and availability limitations imposed by the cold-chain in the global distribution and storage of vaccines. We focused here on DNA vaccination due to the relevance of needle-free vaccines for global health and the need for enhanced DNA vaccination strategies. However, the well-known adaptability of multilayers for incorporation and controlled release of diverse therapeutics[15,46–51] suggests this approach should be applicable to diverse drug delivery applications. Further, the pH-sensitive release-layer strategy employed here is a generalizable approach to create selectively-released multilayer films. While the true potential of any vaccination strategy can only be established in human clinical trials, the data shown here suggest that multilayer tattooing is a promising approach to enhance the efficacy of DNA vaccines, a platform technology with the potential to be applied universally in vaccine development.

Materials and Methods

Materials

(b)PNMP (31:59:10 oNBMA:MMA:PEGMA by mol, 17 kDa), poly-1 (15 kDa), and poly-2 (20 kDa) were synthesized as previously reported.[18,24] AL-11/H-2K^b-peptide-MHC II tetramers were provided by the NIH tetramer core facility.

PLLA microneedle fabrication

PDMS molds (Sylgard 184, Dow-Corning, Midland, Michigan) were prepared using a Clark-MXR-CPA-2010 (VaxDesign Inc., Orlando, Florida). PLLA (IV 1.9 dL/g, Lakeshore Biomaterials) was melted over the molds under vacuum (−25 in. Hg, 200°C, 40 min), and then cooled to −20°C before removal and crystallization at 140°C for 4 hr for solvent resistance.

PNMP release-layer deposition

On Si substrates, 3 wt% PNMP in 1,4-dioxane was deposited using a Specialty Coating Systems P6700 (Indianapolis, Indiana). On PLLA microneedles, 0.25 wt% (b)PNMP was spray deposited as previously described (0.2mL/s, 15 cm range, 10s).[20] Films were dried under vacuum at 25°C for 12 hr. bPNMP release-layers were labeled with Alexafluor-488-conjugated-SAv (10 μg/mL in PBS pH 6.0, Sigma-Aldrich, St. Louis, Missouri).

Polymer multilayer film preparation

LbL films were assembled using a Carl Ziess HMS-DS50 stainer. Films were constructed on Si wafers and PLLA microneedles following deposition of (b)PNMP and photoswitching via UV-irradiation (254 nm, 2.25 mW/cm^2) for 15 min. (PS/SPS) base layers were deposited through alternative immersion into PS (2 mg/mL, Sigma-Aldrich) and SPS (5 mM, Sigma-Aldrich) for 10 min, separated by two 1 min PBS rinses. (PBAE/nucleic acid) multilayers were deposited similarly, alternating 5 min dips in poly-1/2 (2 mg/mL) and either pLUC, pGag, or poly(I:C) (Invivogen, San Diego, California) solutions (1 mg/ml) separated by two 30 sec PBS rinses. Fluorescent pLUC and poly(I:C) were prepared using Cy5 and tetramethyl-rhodamine (TMR) Label-IT reagent (Mirus Bio Corporation, Madison, Wisconsin). All solutions were in PBS, adjusted to pH 5.0. Films were characterized using a Veeco Dektak profilometer and a Zeiss LSM510. Data analysis was performed using Image J. Film loading was determined using a SpectraMax 250 following elution of films in PBS, pH 7.4, 2M NaCl for 24 hours.

In Vitro/In Vivo Delivery

For *in vitro* release experiments, $(PS/SPS)_{20}(PBAE/nucleic\ acid)_{35}$ films were incubated in PBS at 37°C and aliquots were assayed for pLUC or poly(I:C) using picogreen or ribogreen assay kits (Invitrogen). For *in vitro* delivery, coated microneedles were incubated in PBS, pH 7.4 and imaged by confocal microscopy. *In vivo* delivery experiments were performed on anesthetized C57BL/6 mice (Jackson Laboratories, Bar Harbor, Maine) and MHC II-GFP transgenic mice (a gift from Prof. Hidde Ploegh).[26] Ears were rinsed with PBS on the dorsal side and dried before application of microneedle arrays by gentle pressure. Applied microneedles were imaged by confocal. Treated skin was excised and stained with trypan blue for needle penetration. Ears treated with Cy5-pLUC- or TMR-poly(I:C)-coated microneedles (±UV-treatment) were mounted and imaged by confocal. Clearance of fluorescent poly(I:C) and transfection in mice treated with pLUC-coated arrays (±UV-treatment) was measured using an IVIS Spectrum 200 (Caliper Lifesciences, Hopkinton, Massachusetts). For luminescent measurements of pLUC expression, mice were imaged following IP administration of D-luciferin (150mg/kg). For luminescent imaging of MPO-dependent oxidative burst, luminol sodium salt (Santa Cruz Biotech, Santa Cruz, California) was administered IP (250mg/kg) before imaging as previously described.[29] Fluorescence/bioluminescence data was processed using region of interest (ROI) analysis with background subtraction and internal control ROI comparison to untreated skin using the Living Image 4.0 software package (Caliper).

Vaccinations

Animal studies were approved by the MIT IUCAC and animals were cared for in the USDA-inspected MIT Animal Facility under federal, state, local, and NIH guidelines for animal care. Groups of 4 C57Bl/6 mice were immunized with 20 μg pGag and 10 μg poly(I:C) by intramuscular injection (15μl, quadriceps) with or without *in vivo* electroporation (Harvard Apparatus ECM830, 2x60ms pulses, 200V/cm), intradermal injection (15μl, dorsal ear skin, poly(I:C) mixed with free DNA or DNA/poly-1 polyplexes), or by microneedle array (15 min application of $(PS/SPS)_{20}(poly\text{-}1/poly(I:C))_{35}(poly\text{-}1/pGag)_{35}$ on *uv*-PNMP and native-PNMP coated PLLA arrays). To form poly-1/pDNA polyplexes, pDNA was mixed as previously described with PBAE (1:1 ratio by mass) in deionized water and vortexed briefly prior to injection.[52] All animals received the same delivered doses of pGag and poly(I:C); microneedle-delivered dosages were determined by comparison of total eluted pDNA from coated arrays before and after treatment. Frequencies of Gag-specific $CD8^+$ T-cells and their phenotypes were determined by flow cytometry analysis of peripheral blood mononuclear cells following staining with DAPI (live/dead), anti-CD8α, anti-CD44, anti-CD62L, and AL-11/H-$2K^b$-peptide-MHC tetramers. Anti-Gag IgG titers, defined as the dilution of sera at which OD reading was 0.25, were determined by ELISA using SIV-mac251 (My Biosource, San Diego, California) coated plates, and UV-Vis detection of peroxidase conversion of tetramethybenzydine (KPL, Gaithersburg, Maryland) using HRP-conjugated anti-IgG (Jackson Immunoresearch, West Grove, Pennsylvania). To assess recall responses, microneedle-treated animals were challenged with 50 μg intramuscular pGag in the quadriceps and cytokine expression was measured by flow cytometry in peripheral blood mononuclear cells following stimulation with AL11 peptide, treatment with brefeldin A, and staining with DAPI, anti-CD8α, and anti-IFNγ, anti-TNFα.

Ex vivo Macaque Skin Culture and Microneedle Testing

Macaque studies were approved by the Harvard Medical School IACUC. Outbred Rhesus monkeys were housed at New England Primate Research Center. Fresh skin was obtained from the quadriceps of euthanized Rhesus macaques. Skin was mounted on slides and microneedles were applied by gentle pressure. Skin was stained using trypan blue for needle insertion, formaldehyde fixed, and embedded in parrafin for histological sectioning, hemotoxylin and eosin staining, and optical imaging. To assay *ex vivo* transfection, pLUC was injected intradermally (20μg in 10μl PBS) or delivered by microneedle in $(PS/SPS)_{20}(poly\text{-}1/pLUC)_{35}$ multilayers overlying native or *uv*-PNMP. Skin was cultured as previously described[53] and imaged using an IVIS Spectrum after addition of 300 μg luciferin to the culture media. Data analysis was performed as before using the Living Image Software package.

Statistical Analysis

Statistical analysis was performed with Graphpad Prism (La Jolla, California) using two-way analysis of variance or t-test. Values are reported as mean ± s.e.m.

Supplementary Material

Refer to Web version on PubMed Central for supplementary material.

Acknowledgments

This work was supported in part by the Ragon Institute of MGH, MIT, and Harvard, the NIH (AI095109), and the Dept. of Defense (contracts W911NF-07-D-0004). We thank Robert Parkhill and Mike Nguyen (VaxDsign, Inc.) for assistance with microneedle array fabrication. D.J.I. is an investigator of the Howard Hughes Medical Institute.

References

1. Kutzler MA, Weiner DB. DNA vaccines: ready for prime time? Nat. Rev. Genet. 2008; 9:776–788. [PubMed: 18781156]
2. Rice J, Ottensmeier CH, Stevenson FK. DNA vaccines: precision tools for activating effective immunity against cancer. Nat. Rev. Cancer. 2008; 8:108–120. [PubMed: 18219306]
3. Ulmer JB, Wahren B, Liu MA. Gene-based vaccines: Recent technical and clinical advances. Trends Mol. Med. 2006; 12:216–222. [PubMed: 16621717]
4. Sardesai NY, Weiner DB. Electroporation delivery of DNA vaccines: prospects for success. Curr. Opin. Immunol. 2011; 23:421–429. [PubMed: 21530212]
5. Weir E, Hatch K. Preventing cold chain failure: vaccine storage and handling. CMAJ. 2004; 171:1050. [PubMed: 15505266]
6. A. Pruss-Ustun, ER.; Hutin, Y. WHO Environmental Burden of Disease Series. World Health Organization; 2003.
7. Dicko M, et al. Safety of immunization injections in Africa: not simply a problem of logistics. Bull World Health Organ. 2000; 78:163–169. [PubMed: 10743280]
8. Giudice EL, Campbell JD. Needle-Free Vaccine Delivery. Adv. Drug Delivery Rev. 2006; 58:68–89.
9. Bins AD, et al. A rapid and potent DNA vaccination strategy defined by in vivo monitoring of antigen expression. Nat. Med. 2005; 11:899–904. [PubMed: 15965482]
10. Johansen P, et al. Antigen kinetics determines immune reactivity. Proc. Natl. Acad. Sci. U.S.A. 2008; 105:5189–5194. [PubMed: 18362362]
11. Jewell CM, Bustamante LSC, Irvine DJ. In situ engineering of the lymph node microenvironment via intranodal injection of adjuvant-releasing polymer particles. Proc. Natl. Acad. Sci. U.S.A. 2011; 108:15745–15750. [PubMed: 21896725]
12. Prlic M, Hernandez-Hoyos G, Bevan MJ. Duration of the initial TCR stimulus controls the magnitude but not functionality of the CD8+ T cell response. J. Exp. Med. 2006; 203:2135–2143. [PubMed: 16908626]
13. Decher G. Fuzzy nanoassemblies: toward layered polymeric multicomposites. Science. 1997; 277:1232–1237.
14. Hammond PT. Engineering Materials Layer-by-Layer: Challenges and Apportunities in Multilayer Assembly. AIChE J. 2011; 57:2928–2940.
15. Macdonald M, Rodriguez NM, Smith R, Hammond PT. Release of a model protein from biodegradable self assembled films for surface delivery applications. J. Controlled Release. 2008; 131:228–234.
16. MacDonald ML, et al. Tissue integration of growth factor-eluting layer-by-layer polyelectrolyte multilayer coated implants. Biomaterials. 2011; 32:1446–1453. [PubMed: 21084117]
17. Shah NJ, et al. Tunable dual growth factor delivery from polyelectrolyte multilayer films. Biomaterials. 2011; 32:6183–6193. [PubMed: 21645919]
18. Doh J, Irvine DJ. Photogenerated polyelectrolyte bilayers from an aqueous-processible photoresist for multicomponent protein patterning. J. Am. Chem. Soc. 2004; 126:9170–9171. [PubMed: 15281792]
19. DeMuth PC, Su X, Samuel RE, Hammond PT, Irvine DJ. Nano-Layered Microneedles for Transcutaneous Delivery of Polymer Nanoparticles and Plasmid DNA. Adv. Mater. 2010; 22:4851–4856. [PubMed: 20859938]
20. Krogman KC, Lowery JL, Zacharia NS, Rutledge GC, Hammond PT. Spraying asymmetry into functional membranes layer-by-layer. Nat. Mater. 2009; 8:512–518. [PubMed: 19377464]
21. Jewell CM, Zhang J, Fredin NJ, Lynn DM. Multilayered polyelectrolyte films promote the direct and localized delivery of DNA to cells. J. Controlled Release. 2005; 106:214–223.
22. Katz JS, Doh J, Irvine DJ. Composition-Tunable Properties of Amphiphilic Comb Copolymers Containing Protected Methacrylic Acid Groups for Multicomponent Protein Patterning. Langmuir. 2006; 22:353–359. [PubMed: 16378444]

23. Little SR, et al. Poly-Beta amino ester-containing microparticles enhance the activity of nonviral genetic vaccines. Proc. Natl. Acad. Sci. U.S.A. 2004; 101:9534–9539. [PubMed: 15210954]
24. Lynn DM, Langer R. Degradable Poly(Beta-amino esters): Synthesis, Characterization, and Self-Assembly with Plasmid DNA. J. Am. Chem. Soc. 2000; 122:10761–10768.
25. Su X, Kim B-S, Kim Sara R, Hammond Paula T, Irvine Darrell J. Layer-by-Layer-Assembled Multilayer Films for Transcutaneous Drug and Vaccine Delivery. ACS Nano. 2009; 3:3719–3729. [PubMed: 19824655]
26. Boes M, et al. T-cell Engagement of Dendritic Cells Rapidly Rearranges MHC Class II Transport. Nature. 2002; 418:983–988. [PubMed: 12198548]
27. Jewell CM, et al. Release of Plasmid DNA from Intravascular Stents Coated with Ultrathin Multilayered Polyelectrolyte Films. Biomacromolecules. 2006; 7:2483–2491. [PubMed: 16961308]
28. Zhang J, Fredin NJ, Janz JF, Sun B, Lynn DM. Structure/property relationships in erodible multilayered films: influence of polycation structure on erosion profiles and the release of anionic polyelectrolytes. Langmuir. 2006; 22:239–245. [PubMed: 16378427]
29. Gross S, et al. Bioluminescence imaging of myeloperoxidase activity in vivo. Nat. Med. 2009; 15:455–461. [PubMed: 19305414]
30. Soria-Castro I, et al. Cot/tpl2 (MAP3K8) Mediates Myeloperoxidase Activity and Hypernociception following Peripheral Inflammation. J. Biol. Chem. 2010; 285:33805–33815. [PubMed: 20736176]
31. Bechler SL, Lynn DM. Characterization of Degradable Polyelectrolyte Multilayers Fabricated Using DNA and a Fluorescently-Labeled Poly(β-amino ester): Shedding Light on the Role of the Cationic Polymer in Promoting Surface-Mediated Gene Delivery. Biomacromolecules. 2012; 13:542–552. [PubMed: 22224541]
32. Elnekave M, Furmanov K, Hovav A-H. Intradermal naked plasmid DNA immunization: mechanisms of action. Expert Rev. Vaccines. 2011; 10:1169–1182. [PubMed: 21854310]
33. van Drunen Littel-van den Hurk S, Hannaman D. Electroporation for DNA immunization: clinical application. Expert Rev. Vaccines. 2010; 9:503–517. [PubMed: 20450325]
34. Sallusto F, Geginat J, Lanzavecchia A. Central memory and effector memory T cell subsets: Function, generation, and maintenance. Annu. Rev. Immunol. 2004; 22:745–763. [PubMed: 15032595]
35. Greenland JR, et al. Beta-Amino Ester Polymers Facilitate in Vivo DNA Transfection and Adjuvant Plasmid DNA Immunization. Mol. Ther. 2005; 12:164–170. [PubMed: 15963932]
36. Saade F, Petrovsky N. Technologies for enhanced efficacy of DNA vaccines. Expert Rev. Vaccines. 2012; 11:189–209. [PubMed: 22309668]
37. Sullivan SP, et al. Dissolving Polymer Microneedle Patches for Influenza Vaccination. Nat Med. 2009; 16:915–920. [PubMed: 20639891]
38. Zhu Q, et al. Immunization by Vaccine-Coated Microneedle Arrays Protects Against Lethal Influenza Virus Challenge. Proc. Natl. Acad. Sci. U.S.A. 2009; 106:7968–7973. [PubMed: 19416832]
39. Chen X, et al. Improved DNA Vaccination by Skin-Targeted Delivery Using Dry-Coated Densely-Packed Microprojection Arrays. J. Controlled Release. 2010; 148:327–333.
40. Gill HS, Soederholm J, Prausnitz MR, Saellberg M. Cutaneous vaccination using microneedles coated with hepatitis C DNA vaccine. Gene Ther. 2010:811–814. [PubMed: 20200562]
41. Mikszta JA, et al. Improved genetic immunization via micromechanical disruption of skin-barrier function and targeted epidermal delivery. Nat. Med. 2002; 8:415–419. [PubMed: 11927950]
42. Song J-M, et al. DNA Vaccination in the Skin Using Microneedles Improves Protection Against Influenza. Mol. Ther. 20:1472–1480. [PubMed: 22508490]
43. Verstrepen BE, et al. Improved HIV-1 specific T-cell responses by short-interval DNA tattooing as compared to intramuscular immunization in non-human primates. Vaccine. 2008; 26:3346–3351. [PubMed: 18467010]
44. Denet A-R, Vanbever R, Preat V. Skin electroporation for transdermal and topical delivery. Adv. Drug Delivery Rev. 2004; 56:659–674.

45. Wallace M, et al. Tolerability of Two Sequential Electroporation Treatments Using MedPulser DNA Delivery System (DDS) in Healthy Adults. Mol. Ther. 2009; 17:922–928. [PubMed: 19277016]

46. Boudou T, Crouzier T, Ren K, Blin G, Picart C. Multiple Functionalities of Polyelectrolyte Multilayer Films: New Biomedical Applications. Adv. Mater. 2010; 22:441–467. [PubMed: 20217734]

47. Dimitrova M, et al. Sustained delivery of siRNAs targeting viral infection by cell-degradable multilayered polyelectrolyte films. Proc. Natl. Acad. Sci. U.S.A. 2008; 105:16320–16325. [PubMed: 18922784]

48. Jessel N, et al. Multiple and time-scheduled in situ DNA delivery mediated by Î²-cyclodextrin embedded in a polyelectrolyte multilayer. Proc. Natl. Acad. Sci. U.S.A. 2006; 103:8618–8621. [PubMed: 16735471]

49. Kim B-S, Park SW, Hammond PT. Hydrogen-Bonding Layer-by-Layer-Assembled Biodegradable Polymeric Micelles as Drug Delivery Vehicles from Surfaces. ACS Nano. 2008; 2:386–392. [PubMed: 19206641]

50. Kim B-S, Smith RC, Poon Z, Hammond PT. MAD (Multiagent Delivery) Nanolayer: Delivering Multiple Therapeutics from Hierarchically Assembled Surface Coatings. Langmuir. 2009; 25:14086–14092. [PubMed: 19630389]

51. Lynn DM. Peeling back the layers: controlled erosion and triggered disassembly of multilayered polyelectrolyte thin films. Adv. Mater. 2007; 19:4118–4130.

52. Akinc A, Anderson DG, Lynn DM, Langer R. Synthesis of Poly(Beta-Amino Ester)s Optimized for Highly Effective Gene Delivery. Bioconjugate Chem. 2003; 14:979–988.

53. Stoitzner P, et al. Migration of Langerhans cells and dermal dendritic cells in skin organ cultures: augmentation by TNF-α and IL-1β. J. Leukocyte Biol. 1999; 66:462–470. [PubMed: 10496317]

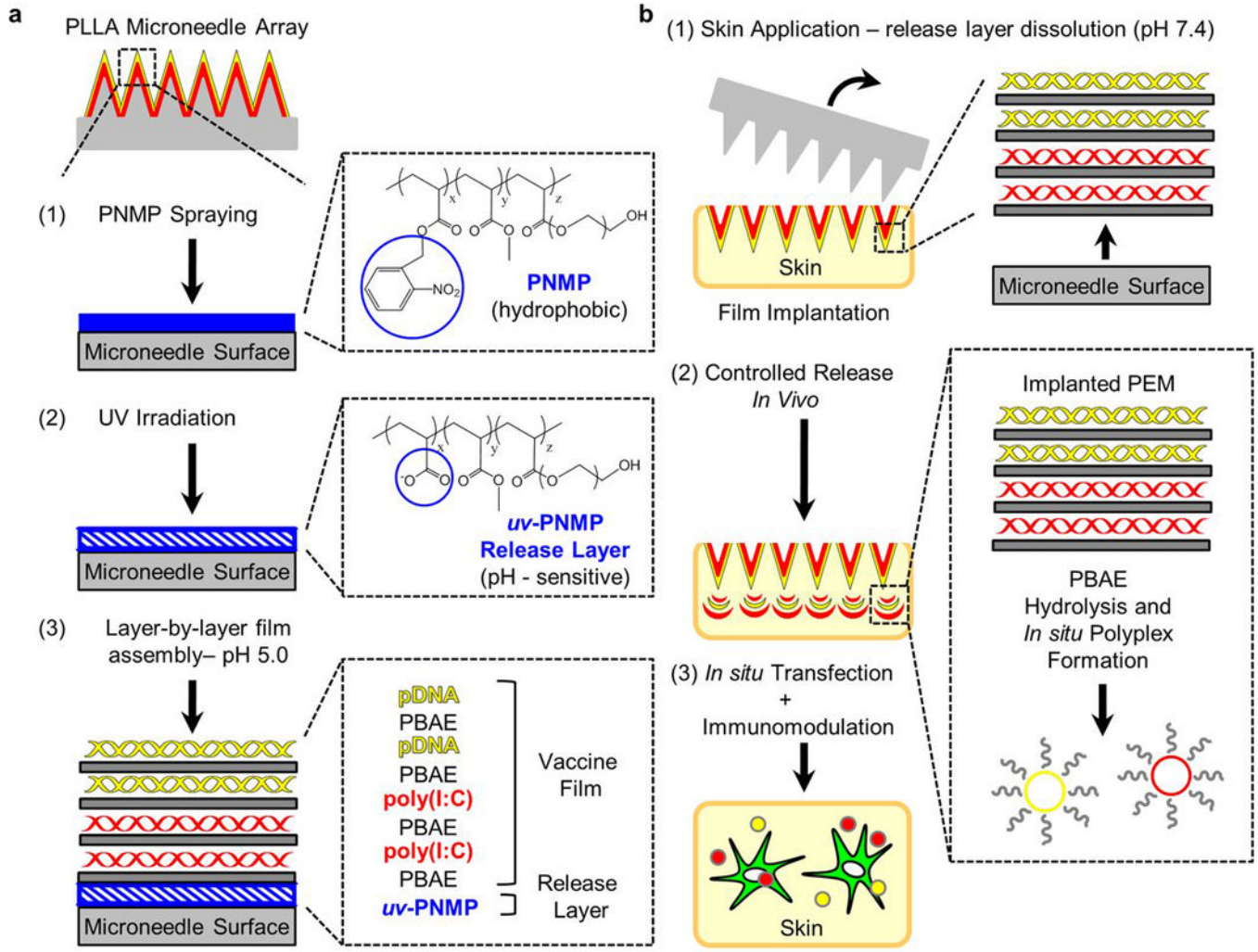

Figure 1. Design of quick-release vaccine-loaded microneedle coatings

a, Schematic view of release-layer-mediated multilayer tattooing strategy using coated microneedles: (1) PLLA microneedles are coated with PNMP release-layer films through spray deposition; (2) UV-irradiation imparts pH-sensitive aqueous solubility to the PNMP film, forming a *uv*-PNMP 'release-layer'; (3) Overlying multilayer films containing nucleic acids are constructed using LbL deposition at pH 5.0. **b,** Mechanism of action for multilayer tattooing: (1) Microneedle application to skin and exposure to interstitial fluid gives rapid release-layer dissolution, mediating overlying film delamination and retention in skin following microneedle removal; (2) Implanted films provide sustained release of nucleic acids through hydrolytic PBAE degradation and release of *in situ*-formed PBAE/nucleic acid polyplexes; (3) released polyplexes mediate local transfection and immune modulation in the tissue.

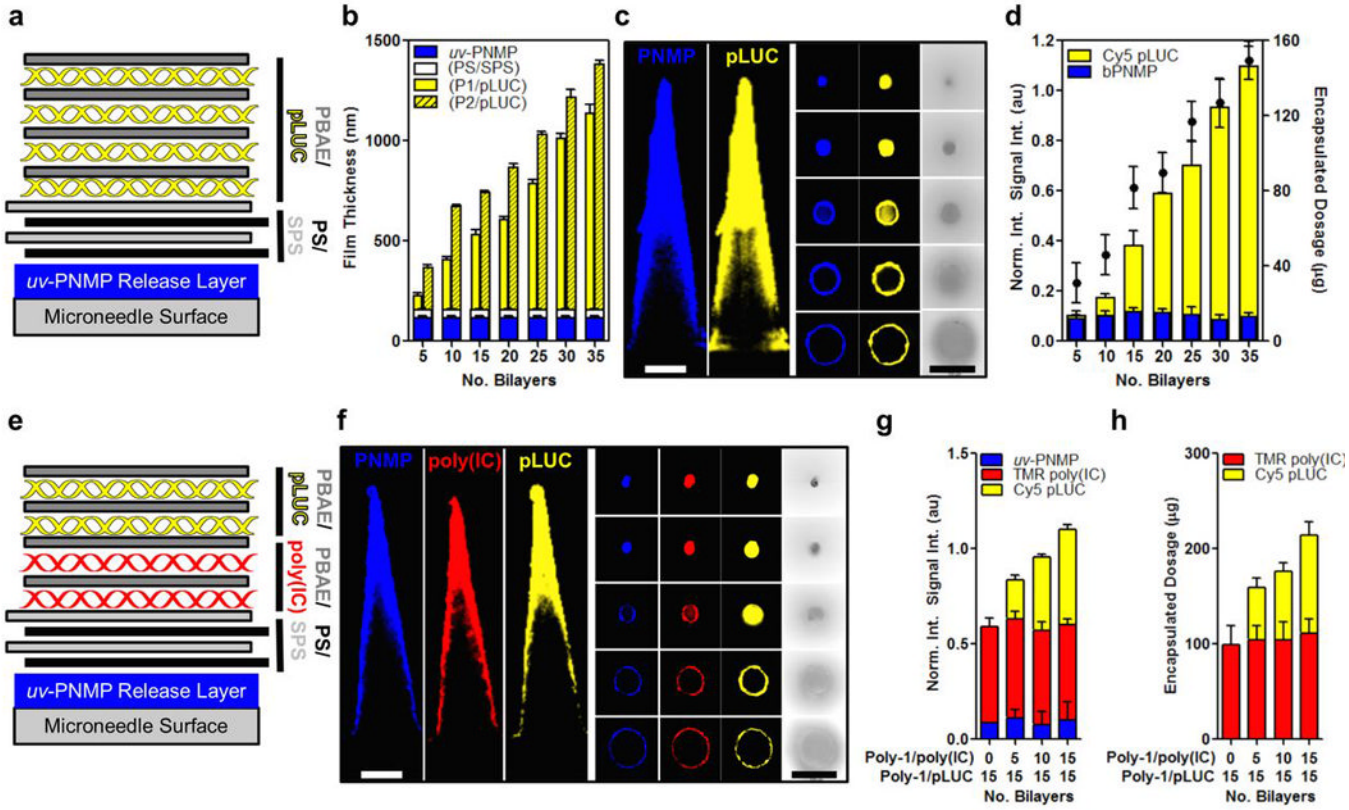

Figure 2. LbL assembly of microneedle coatings carrying DNA, immunostimulatory RNA, and transfection agents

a, Film architecture for (*uv*-PNMP)(PS/SPS)$_n$(PBAE/pLUC)$_n$ multilayers. **b,** Growth of (poly-1/pLUC)$_n$ and (poly-2/pLUC)$_n$ multilayers assembled onto (*uv*-PNMP)(PS/SPS)$_{20}$ films on silicon substrates as a function of the number of deposited (PBAE/pLUC) bilayers as measured by surface profilometry. **c,** Representative confocal images of PLLA microneedles coated with (SAv488-bPNMP)(PS/SPS)$_{20}$(poly-1/Cy5-pLUC)$_{35}$ films (left – transverse optical sections, right – lateral sections, 100µm *z*-intervals, scale bars 200 µm. (blue – Sav488-*uv*-bPNMP, yellow – Cy5-pLUC). **d,** Quantification of Cy5-pLUC and Sav488-bPNMP incorporated into (SAv488-bPNMP)(PS/SPS)$_{20}$(poly-1/Cy5-pLUC)$_n$ films on microneedles through confocal fluorescence intensity analysis (left axis, n = 15) and measurement of total DNA recovered from dissolved films (right axis, n = 3). **e,** Film architecture for (*uv*-PNMP)(PS/SPS)$_{20}$(Poly-1/pLUC)$_n$(Poly-1/poly(I:C))$_n$ multilayers. **f,** Representative confocal images of microneedles coated with (SAv488-*uv*-bPNMP)(PS/SPS)$_{20}$(poly-1/TMR-poly(I:C))$_{15}$(poly-1/Cy5-pLUC)$_{15}$ films (left – transverse sections, right – lateral sections, 100µm z-interval, scale 200 µm. (blue – Sav488-*uv*-bPNMP, yellow – Cy5-pLUC, red – TMR-poly(I:C)). **g, h,** Quantification of Cy5-pLUC, TMR-poly(I:C), and SAv488-bPNMP incorporated into (SAv488-bPNMP)(PS/SPS)$_{20}$(poly-1/TMR-poly(I:C))$_n$(poly-1/Cy5-pLUC)$_n$ films on microneedles through confocal fluorescence intensity analysis (**g,** n = 15) and measurement of total nucleic acids recovered from dissolved films (**h,** n= 3).

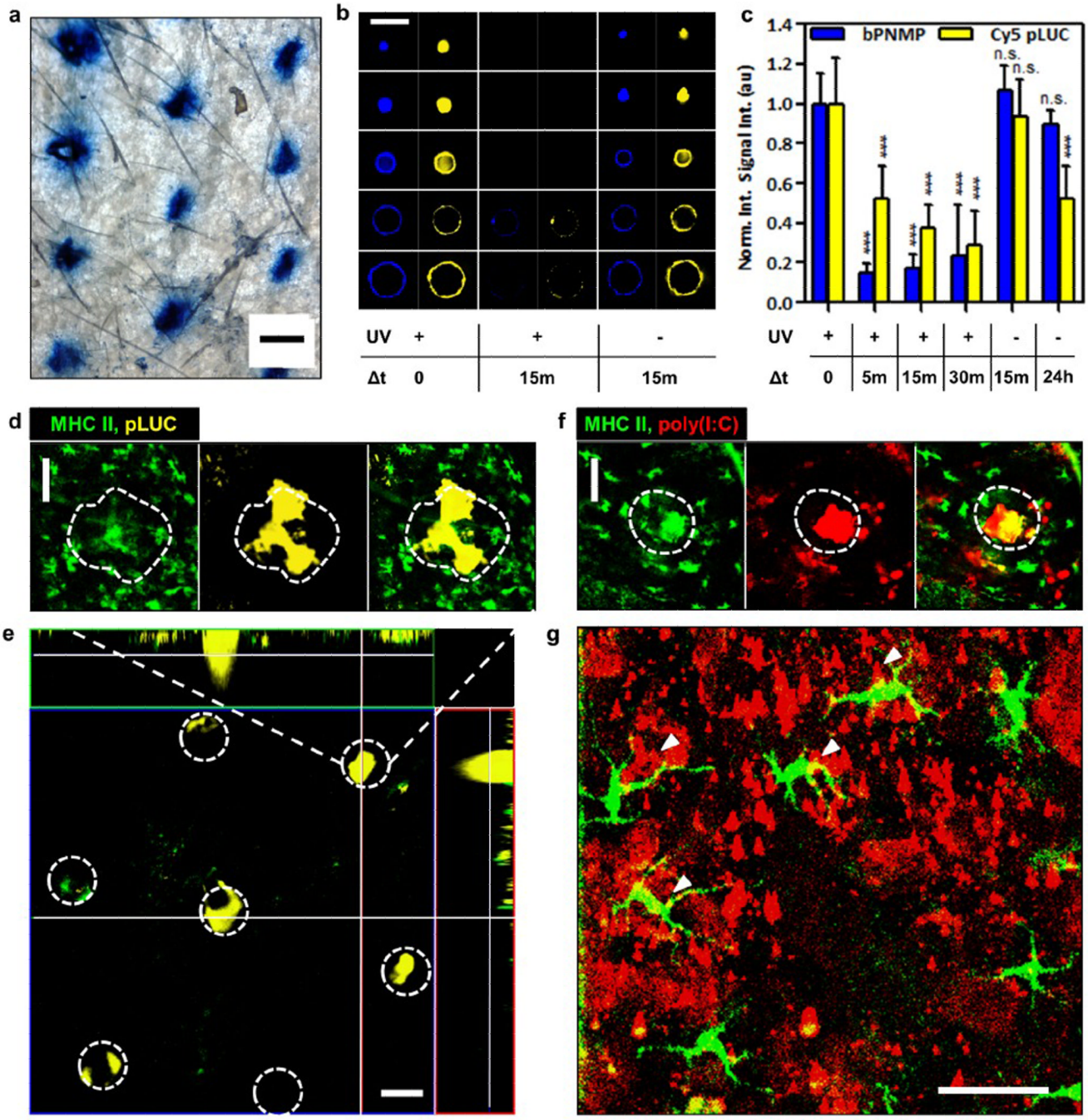

Figure 3. PNMP release-layers promote rapid implantation of multilayer films at microneedle penetration sites *in vivo*

a, Optical micrograph of ear skin stained with trypan blue to reveal epidermal penetration following PLLA microneedle application (scale bar 500μm). **b,** Representative confocal images of (SAv488-bPNMP)(PS/SPS)$_{20}$(poly-1/Cy5-pLUC)$_{35}$-coated PLLA microneedles with or without UV sensitization of the PNMP layer (Blue - Sav488-bPNMP; yellow - Cy5-pLUC), before application, or after 15 min application to murine ear skin (lateral sections, 100 μm *z*-interval, scale bar 200 μm). **c,** Quantitation of confocal fluorescence intensities (*n* = 15) showing loss of Sav488-*uv*-bPNMP and Cy5-pLUC films from coated microneedles upon application to skin, dependent on UV-induced photo-switching of the PNMP layer

solubility. ***, $p < 0.0001$, analyzed by unpaired t-test. **d,** Representative confocal image of treated murine skin showing film implantation after 15 min (green, MHC II-GFP; yellow, Cy5-pLUC; penetration site outlined, scale bar 100μm). **e,** *x-y/x-z/y-z* confocal images showing depth of Cy5-pLUC film deposition after 15 minute microneedle application (green, MHC II-GFP; yellow, Cy5-pLUC; penetration sites outlined, scale bar 200μm). **f,** Representative confocal image of treated murine skin showing TMR-poly(I:C) film implantation after 15 min microneedle application (green, MHC II-GFP; red, TMR-poly(I:C); penetration site outlined, scale bar 100 μm). **g,** Colocalization and uptake of TMR-poly(I:C) by MHC II-GFP$^+$ LCs at microneedle insertion site 24 hrs following film implantation (green, MHC II-GFP; red, TMR-poly(I:C); yellow, overlay, scale bar 50 μm).

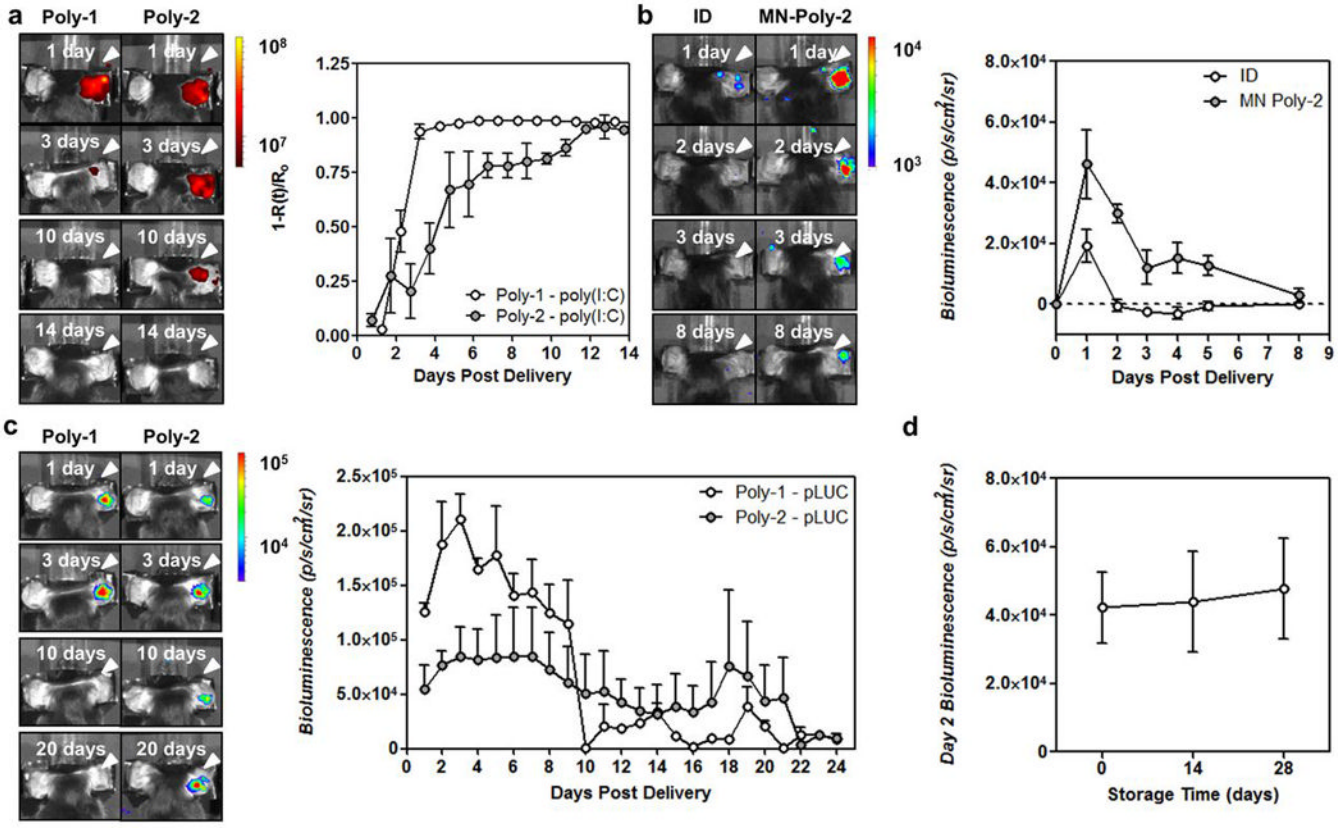

Figure 4. Implanted films control the physical and functional persistence of pDNA and poly(I:C) *in vivo*

a, Representative whole-animal fluorescence images showing TMR-poly(I:C) retention at the application site and quantitative analysis of normalized total fluorescence R(t) relative to initial fluorescence R_o from groups of animals (n = 3) over time following 15 min application of PLLA microneedles coated with (*uv*-PNMP)(PS/SPS)$_{20}$(PBAE/TMR-poly(I:C))$_{35}$ multilayers containing poly-1 or poly-2 as the PBAE component. **b,** Representative whole-animal luminescent images and quantitative analysis of luminol signal from MPO-dependent oxidative burst in activated phagocytes at the treatment site over time following intradermal injection of 10 μg poly(I:C) or 15 min application of PLLA microneedles coated with (*uv*-PNMP)(PS/SPS)$_{20}$(Poly-2/poly(I:C))$_{35}$ multilayers. **c,** Representative whole animal bioluminescence images of pLUC expression at the application site and mean bioluminescence intensity over time following 15 minute application of microneedles coated with (*uv*-PNMP)(PS/SPS)$_{20}$(PBAE/pLUC)$_{35}$ multilayers containing poly-1 or poly-2 as the PBAE component. **d,** Mean bioluminescent intensity on day 2 following 15 min application of microneedles coated with (*uv*-PNMP)(PS/SPS)$_{20}$(Poly-1/pLUC)$_{35}$ multilayers stored dry at 25°C for 0, 14, or 28 days.

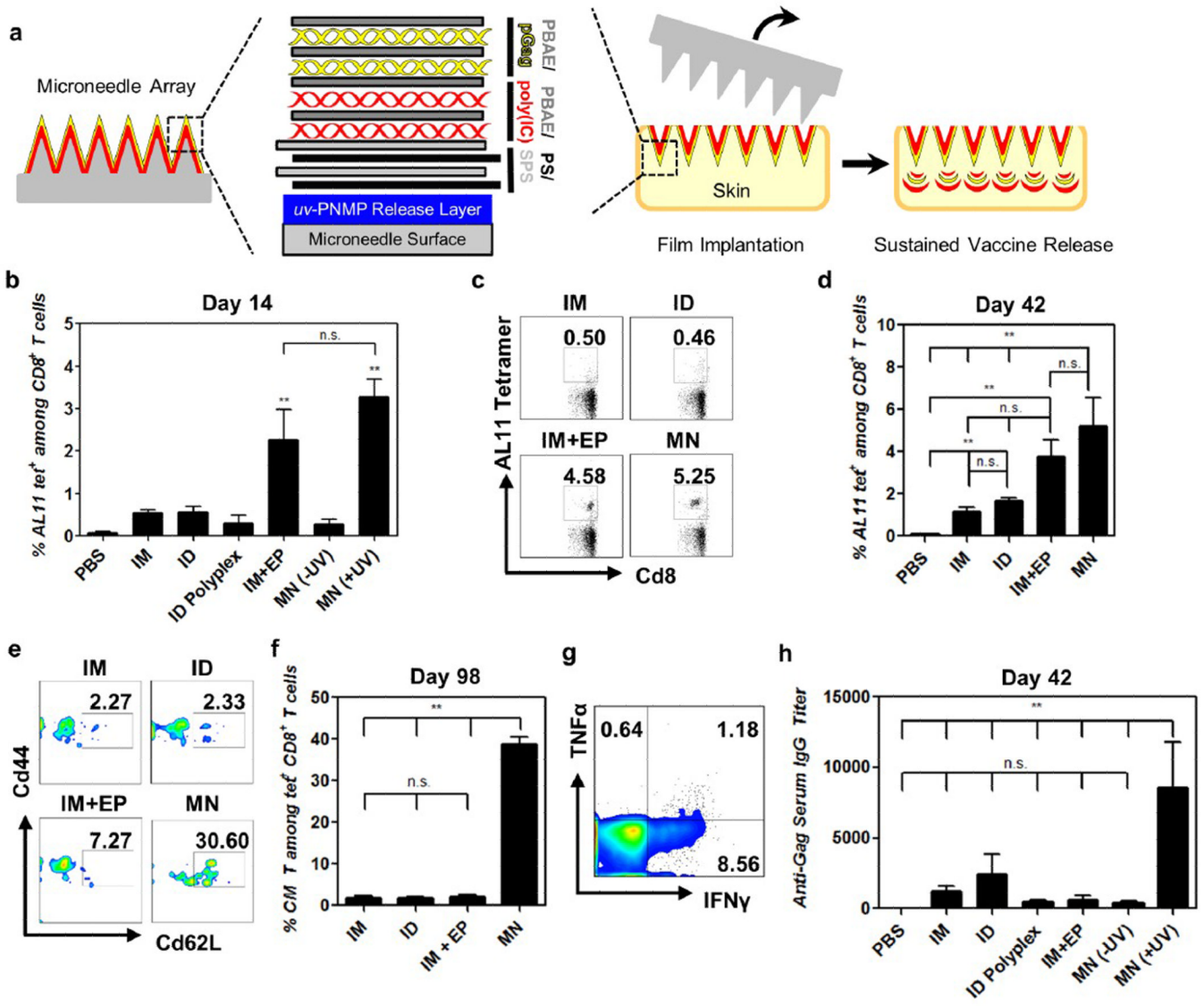

Figure 5. Microneedle tattooing with multilayer films carrying pDNA and poly(I:C) generates potent cellular and humoral immunity against a model HIV antigen

a, C57Bl/6 mice (n = 4 mice/group) were immunized with 20 μg pGag and 10 μg poly(I:C) on days 0 and 28 intramuscularly (with or without electroporation (EP)) in the quadriceps, intradermally in the dorsal ear skin (with free pGag or pGag/poly-1 polyplexes, ID ± Polyplex), or by 15 minute application of $(PNMP)(PS/SPS)_{20}(poly\text{-}1/poly(I:C))_{35}(poly\text{-}1/pLUC)_{35}$–coated microneedles without or without UV priming of the PNMP release-layer (MN ± UV) to the dorsal ear skin. **b-d,** Frequency of Gag-specific $CD8^+$ T-cells in peripheral blood assessed by flow cytometry analysis of $tetramer^+$ $CD8^+$ T-cells. Shown are mean $tetramer^+$ values from **b,** day 14 and **c,** representative cytometry plots from individual mice and **d,** mean $tetramer^+$ values from day 42. **e-f,** Analysis of T-cell effector/central memory phenotypes in peripheral blood by CD44/CD62L expression of $tetramer^+$ cells from peripheral blood. Shown are **e,** representative cytometry plots from individual mice at day 49 and **f,** mean percentages of $tetramer^+CD44^+CD62L^+$ among $CD8^+$ T cells at day 98. **g,** Mice immunized with microneedles were recalled on day 105 by IM injection of 50 μg pGag, and assessed for cytokine production on *ex vivo* restimulation with AL11 peptide on

day 112. Shown is representative flow cytometry analysis of IFN-γ/TNF-α-producing $CD8^+$ T-cells. **h,** Enzyme-linked-immunosorbent assay analysis of total Gag-specific IgG in sera at day 42. **, $p < 0.005$, analyzed by two-way ANOVA.

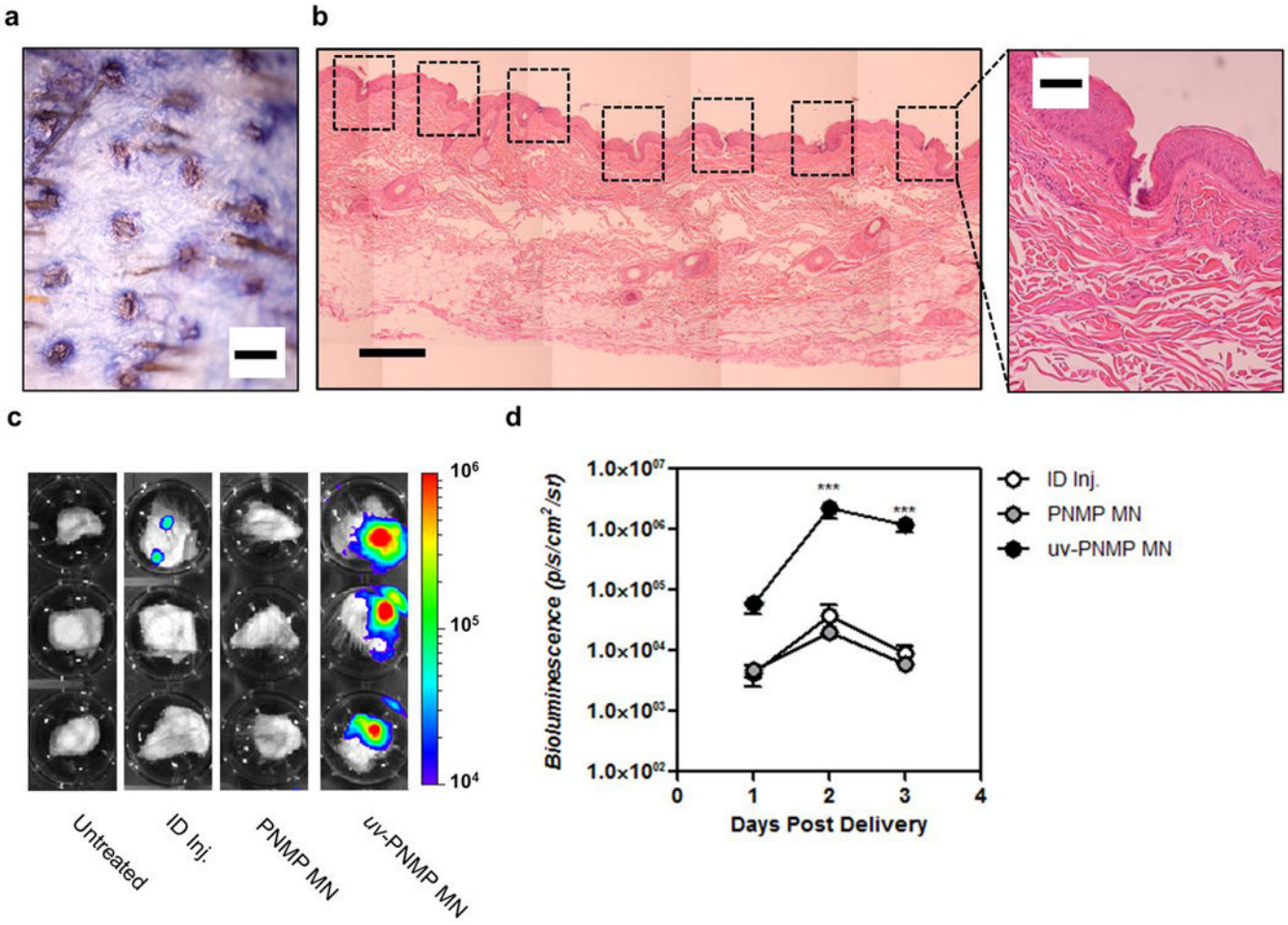

Figure 6. Multilayer tattooing enhances transfection in non-human primate skin

a, Optical micrograph of macaque quadriceps skin showing microneedle penetration pattern stained using trypan blue (scale bar 500μm). **b,** Histological section of microneedle-treated macaque skin showing epidermal disruption at microneedle insertion sites (boxed, left, scale bar 500μm; right, scale bar 100μm). **c,** Bioluminescence images of luciferase expression 2 days following pLUC delivery by ID injection or microneedle tattooing with $(PS/SPS)_{20}(poly\text{-}1/pLUC)_{35}$ films from either *uv*-PNMP- or non-irradiated PNMP-coated microneedles following a 15 minute application. **d,** Quantification of total bioluminescent signal in cultured skin tissue explants 1, 2, and 3 days following treatment. ***, $p < 0.0001$, analyzed by unpaired t-test.